

Gamma Putty shielding effect in megavoltage photon beam

Aime M Gloi

Department of Radiation Oncology, HSHS, Green Bay, USA

Received August 26, 2016; Revised April 3, 2017; Accepted May 15, 2017; Published Online June 25, 2017

Original Article

Abstract

Purpose: Traditionally, lead and Cerrobend have been employed for field shaping in radiation therapy. Lately, another shielding material called Gamma Putty has emerged. The objective of this report is to examine its dosimetric and shielding characteristics in megavoltage photon beam. **Methods:** All measurements were carried out in a dual energy linac. Data were collected using a calibrated ionization chamber. Percent transmission, linear attenuation, and field size dependence were evaluated for open square fields ($4 \times 4 \text{ cm}^2$ to $10 \times 10 \text{ cm}^2$) defined by collimator jaws and for different Gamma Putty thicknesses ($t = 0, 0.3, 0.5, 1.0, 1.5, 2.0$, and 2.5 cm) at 6 and 18 MV photon beams. The measurements were performed both in air using appropriate acrylic buildup cap and in solid water. **Results:** The Gamma Putty tray factor (GPTF) increased steadily with field size for both 6 and 18 MV. It was characterized by a half value thickness (HVT) of 2.513 ± 0.101 and $2.855 \pm 0.024 \text{ cm}$ for 6 and 18 MV, respectively. The reduction in surface dose was about 6%, 14.5%, 22%, 36.37%, and 54% for 6 MV and 2.75 %, 9.36 %, 16.25 %, 28.95 %, and 44.47 % for 18 MV for Gamma Putty thicknesses of 0.3, 0.5, 1.0, 1.5, 2.0, and 2.5 cm. **Conclusion:** The result of Gamma Putty shielding on the photon beam output increases with thickness, beam energy, and field size. Therefore, clinical use of Gamma Putty tray factors should be tailored for all thicknesses, beam energies, and field sizes.

Keywords: Gamma Putty, Tray factor, Linear attenuation, Surface dose.

1. Introduction

The purpose of radiotherapy treatment is to deliver dose to the tumor and curtail dose to the surrounding normal tissue by sometimes using beam modifiers. Based on several reports, Lead and cerrobend blocks have been commonly and predominantly used.^{1,2} Several authors have described a wide range use of block applications. Purdy *et al.*³ used a gonadal shield based cerrobend in the pelvic irradiation of males to reduce the gonadal dose to about 1.5 – 2.5% of the given dose. Sohn *et al.*⁴ employed a mobile shield to decrease the scatter dose to the contralateral breast from the linear accelerator by a factor of 3 to 4. In the head and neck treatment radiation, stents were utilized to protect healthy tissues,^{5,6} whereas in the mantle instance, MLC leaves were moved in or out to get the required shape in some cases.⁷

Nevertheless, these shielding blocks cannot always conform exactly to the patient anatomy and region of interest. They experienced variable thickness consistency and are hard to plan and align effectively on the patient. To maximize a good shielding material, some

properties are desirable. They included high atomic number and attenuation coefficient so as to absorb a radiation, and a low melting point. The shielding material must be malleable for better conformity, inexpensive, and easily disposable for environment concerns. Recently, a material called Gamma Putty that has been used in the industrial setting for different purposes such as shielding cable tray penetrations around pipes and radiographic film masking to prevent radiation scatter has been wooing as an alternative for lead and cerrobend for many reasons. The Putty is lead free, malleable, reusable, and can be thinned, thickened, reshaped to follow patient anatomy. As soon as, the wanted shield is made and wrapped in plastic, it can be used for the whole treatment schedule. Furthermore, when treating small lesions electron cutouts are often used to shape the beam to the tumor and sparing normal tissue surrounding the tumor. The drawback of using a cutout is that the field size is smaller and to some extent inadequate for treatment, resulting in under dosage of lateral tissues. Several important dosimetric parameters for controlling the dose at extended distances, such as

Corresponding author: Aime M Gloi; Department of Radiation Oncology, HSHS, Green Bay, USA.

Cite this article as: Gloi A. Gamma Putty shielding effect in megavoltage photon beam.. *Int J Cancer Ther Oncol.* 2017; 5(1):515. DOI: 10.14319/ijcto.51.5

the percent depth dose, flatness, penumbra, and uniformity, are greatly affected. In addition, a slight offset of the field can also result in a large dose displacement from the region of interest. These facts have been emphasized by several studies.^{1,2,3,4} Again, from dosimetric perspective lead or cerrobend are believed to be a better skin collimator. However, Gamma Putty as a skin collimator is more easily fabricated and required no specific tools than lead or Cerrobend. The goal of this study is to evaluate the dosimetric and shielding properties of Gamma Putty in megavoltage radiation therapy. The clinical motivation of this study is many folds:

1.1. Potential

In this report the effects of Gamma Putty shielding blocks on incident photon beams of 6 and 18 MV energies were examined and its clinical potential in radiotherapy evaluated. Gamma Putty could be an additional arsenal in beam shaping and shielding of healthy tissues surrounding the tumor site.

1.2. Characteristics

In short, Gamma Putty is a non-hardening material that has been used during nuclear reactor maintenance as temporary gamma radiation shielding. It is non-toxic, malleable, and readily available commercially. It is very pliable and yet has enough consistency to hold its shape after placement. The material can be reused for many radiotherapy sessions and is environmentally friendly since it is Lead free. It necessitates no special tools or techniques to create patient shields and easier to adapt to patient body contour. It is loaded with 90 % bismuth with high atomic number ($Z = 83$), thereby useful to shield critical structures as suggested by several reports,^{8,9,10} arguing for the shielding properties of high Z materials.

1.3. Clinical applications

The potential clinical application of Gamma Putty is tremendous. From small field ranging from tip of the nose to eye lesion, it could be broaden to include large fields that accommodate the protection of intraoral head and neck sites, lungs in the case of Mantle field for Hodgkin's disease, and kidneys for total body irradiation. However, further study is required to assess the dose distribution behind the protected area, as well as tailoring Gamma Putty thickness for individual cases.

2. Methods and Materials

The Gamma Putty (shieldwerx, Rio Rancho, New Mexico, USA) shielding blocks were produced from Iron poly putty (LDPE) loaded with 90% of Bismuth and a high hydrogen content gear to slow fast neutrons to thermal neutrons with a density of 3.8 g/cc. In this study, the Gamma Putty blocks were in circular shapes with different thicknesses. They were mounted on the blocking tray at 67.2 cm distance from source target of

the Trilogy ((Varian Medical systems, Palo Alto, USA) delivering both 6 and 18 MV photon beams.

2.1. Gamma Putty tray factors (GPTF)

A photon attenuation characteristic of Gamma Putty was assessed for 6 and 18 MV megavoltage photon beams using variable field sizes (4×4 , 5×5 , 6×6 , 8×8 , 9×9 , and 10×10 cm²) and normalized to a 10×10 cm² field size. A PTW Farmer chamber of 0.6 cc (PTW Freiburg, Germany) chamber was placed in air to evaluate GPTF. The charge was collected by the ionization chamber and was measured with an electrometer Model 206 (CNMC, Nashville, TN, USA) using a bias potential of to -300 V across the chamber. All measurements were performed with the detector set isocentrically and perpendicular to central axis of the beam. Two acrylic build up caps with diameter 1.3 cm and 3.5 cm were used for 6 and 18 MV photon beams respectively. The thickness of the build-up cap in each case was sufficiently large enough to provide maximum dose at the chamber. The radiation transmission factor of Gamma Putty (GPTF) is defined here as the ratio of the charge measured with and without Gamma Putty in the beam, for the same number of monitor units:

$$GPTF(c) = \frac{D_{GP}(d_{max}, c, f)}{D_{open}(d_{max}, c, f)} \quad (1)$$

where, c is the collimator opening and distance from the source (f).

2.2. Percent ionization depth measurement

In order to evaluate change of depth dose distribution by the Gamma Putty, percentage ionization depths were measured for several Gamma Putty thicknesses (0.3, 0.5, 1.0, 1.5, 2.0, and 2.5 cm). Thus, analyzing the dosimetric impact of beam are hardening, softening, scattering, and electron contamination. The measurements were performed in solid water Model 458 (CNMC, Nashville, TN, USA). The field size was 10×10 cm², and the source to surface distance (SSD) was set at 100 cm. 100 monitors unit (MU) were given each time.

2.3. Linear attenuation coefficient determination

The linear attenuation coefficients value was measured at 6 and 18 MV photon beams via a Farmer type ionization chamber. These were performed variable field sizes (4×4 , 5×5 , 6×6 , 8×8 , 9×9 , and 10×10 cm²) moderated by Gamma Putty with thickness of (0.3, 0.5, 1.0, 1.5, 2.0, 2.5 cm) placed on accessory tray and performed in air with appropriate buildup cap to reduce the impact of phantom scatter.

3. Results and Discussion

3.1. Gamma Putty Blocks

In this study, the effect of Gamma Putty shielding block on relative dose in various field sizes and thicknesses

were analyzed. Six blocks of variable thicknesses (0.3, 0.5, 1.0, 1.5, 2.0, and 2.5 cm) were utilized to assess the dose distribution in various field sizes shielded by the Gamma Putty (Figures 1a and b). The GPTF as a function of field size is illustrated in Figures 2a and b for 18 and 6 MV photon beam, respectively. GPTF (Tables 1a and b) was generated based on measurements achieved in air



Figure 1a: Variable Gamma Putty thickness in a plastic wrap.

using Farmer type ionization chambers placed on the beam central axis at the reference depth of d_{max} in acrylic build up caps that provided charged particle equilibrium. The reference depths for 6 and 18 MV photon beams are 1.3 and 3.5 cm respectively.

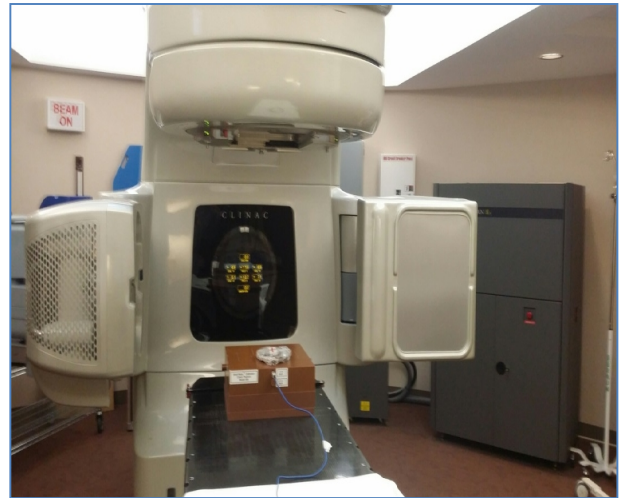


Figure 1b: Measurement with Gamma Putty on the linac using a solid water and ion chamber.

Table 1a: Variations of GPTF for 6 MV photon beams as a function of field size and Gamma Putty thickness.

Field Size (cm)	Gamma Putty thickness (cm)					
	0.3	0.5	1.0	1.5	2.0	2.5
10	0.874439	0.815503	0.734145	0.661755	0.588085	0.506726
9	0.874838	0.817121	0.73476	0.661479	0.588846	0.505837
8	0.874016	0.815617	0.733596	0.660105	0.586614	0.503937
7	0.874335	0.814495	0.732048	0.65891	0.585106	0.50266
6	0.874409	0.81499	0.731938	0.657664	0.584065	0.501688
5	0.874313	0.81456	0.731456	0.656593	0.583104	0.500687
4	0.873603	0.813547	0.729749	0.655726	0.581704	0.499302

Table 1b: Variations of GPTF for 18 MV photon beams as a function of field size and Gamma Putty thickness.

Field Size (cm)	Gamma Putty thickness (cm)					
	0.3 cm	0.5 cm	1.0 cm	1.5 cm	2.0 cm	2.5 cm
10	0.91342	0.85974	0.8	0.707359	0.641558	0.535931
9	0.916667	0.859319	0.802867	0.706093	0.641577	0.533154
8	0.915663	0.857275	0.802595	0.704356	0.639481	0.53012
7	0.914587	0.856046	0.801344	0.702495	0.636276	0.527831
6	0.91517	0.856287	0.800399	0.702595	0.634731	0.525948
5	0.9158	0.856549	0.799376	0.701663	0.634096	0.524948
4	0.915767	0.856371	0.798056	0.699784	0.632829	0.523758

Figures 2a and b shows the GPTF as a function of field size for variable Gamma Putty block thickness for both 6 and 18 MV. The figures revealed that GPTF increases steadily with increasing field size and decreasing Gamma Putty thickness for both 6 and 18 MV photons beam. This is due to increased scatter contribution, for all Gamma Putty thicknesses at two energies. However, there is a minor GPTF changes as a function of field size for the same Gamma Putty thickness, which is systematically higher for 18 MV. The changes at 18 MV increase with field size and a 50.6% difference was noticeable for a 2.5 cm Gamma Putty block. However, behind a block of 0.3 cm thickness, the difference was evaluated at 12.55%. The trend could be described by linear regression fits that depended on Gamma Putty thickness as illustrated in Table 2. The observed effect was perhaps due to the secondary electron contamination of the photon beam especially at 18 MV. There was a strong relationship between field size and GPTF as Gamma Putty thickness increases. For instance, for 2.5 cm, $R^2 = 0.997$ and 0.963 for 6 and 18 MV, respectively. In fact, dose received by a point in air shielded by Gamma Putty blocks included contribution from the primary photon, scattered photons produced, and electron contamination derived from the Gamma Putty itself. This effect is enhanced by increasing field size, and energy (18 MV). Also, 90 % of the Gamma Putty is loaded with Bismuth component of atomic number $Z = 83$. Both attenuation and scattering of the photon beam by the Gamma Putty occurred due to pair production.

Table2: Linear regression R^2 for Gamma at variable thicknesses and field sizes

Thickness (mm)	6 MV	18 MV
3	0.404	0.126
5	0.634	0.704
10	0.903	0.446
15	0.988	0.960
20	0.950	0.951
25	0.997	0.963

Figure 3a displayed the measured relative ionization depth dose curves in solid water phantom at 18 and 6 MV photon beam, respectively for open beam. Similarly, Figures 3b and c illustrated the changes in relative percent ionization depth dose in solid water for various Gamma Putty thicknesses. This will be translated in notable variation in 18 MV compared to 6 MV. For 6 MV, the curve slopes positions are deeper than the d_{max} , and decreased because of the beam hardening effect as Gamma Putty thickness increases. For instance, for 2.5 cm Gamma Putty thickness, the difference in the relative percent ionization dose at a depth of 10 cm photons was 55.6%, and 58.55% for 6 and 18 MV photons beams, respectively. Furthermore, a small separation of the curves is noticeable at depths higher than 10 cm, denoting induced Gamma Putty beam hardening. These curves are comparable to the open beam field for both 6 and 18 MV. Nevertheless, Figure 3b does not reveal any

effect at depth of Gamma Putty contaminant electrons. Some reports echoed the same results using Cerrobend compensators on a 6 MV photon beam and suggested that compensators do not significantly impact the percent depth dose characteristics.^{11,12} On the other hand, Figure 3c revealed that at 18 MV the Gamma Putty produced a beam softening at depth that rises as Gamma Putty thickness increased. This is due to pair production from the Gamma Putty. The resulting percent ionization decreases at 15cm depth and reaches 50% for the 2.5 cm block thickness. Conversely at 6 MV, Gamma Putty affects the dose in the build-up region indicating the presence of Gamma Putty scattered photons or contaminant electrons in the beam.

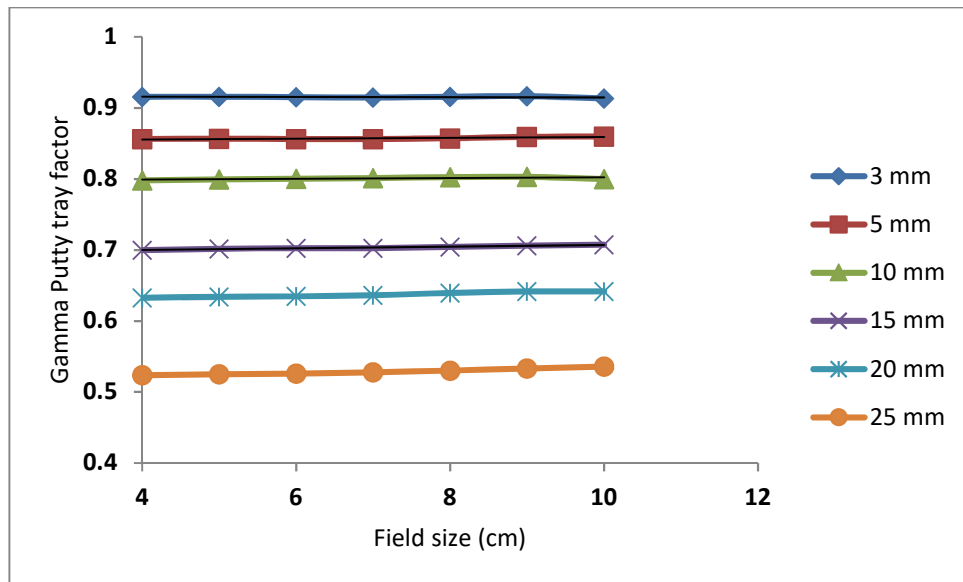
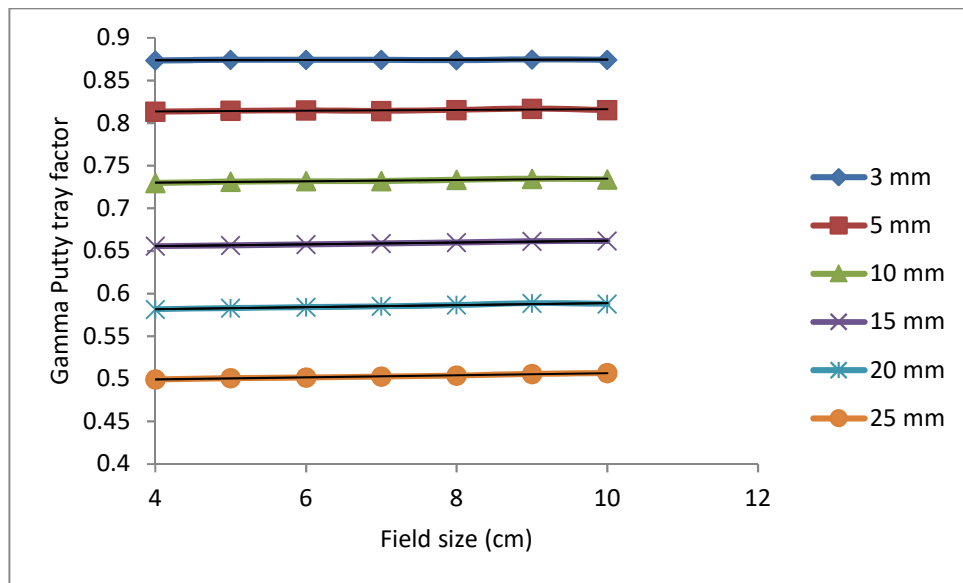
3.2. Evaluation of the attenuation coefficient of Gamma Putty

The effects of radiation beam attenuation for 6 and 18 MV photon beam are illustrated in Table 3. The half value thickness (HVT) and Tenth value thickness (TVT) are determined based on an exponential fitting. An example is displayed in Figures 4a and b for $10 \times 10 \text{ cm}^2$ field size with a good linear regression coefficient for 6 and 18 MV photon beam, respectively. This is translated by a coefficient of variation of 4.0% and 0.8% for 6 and 18 MV, respectively. The difference observed between HVT suggested a strong beam energy hardening dependent. The evaluation of linear attenuation coefficient in this study is similar to that of Du Plessis *et al.*¹³

3.3. Evaluation Off-axis relative dose

Off-axis relative percent ionization dose profiles are shown in Figures 5a and b for 6 and 18 MV photon beam, respectively. Only small infield differences, 2% in some instances are accounted for. This difference in out of field photon dose was higher at 18 MV. The increase in percentage skin dose due to the Gamma Putty is greater at central axis (CAX) with an estimate reduction of 5–10% from the CAX out to the field edge. This may be due to the lateral scatter of electron contamination from the Gamma Putty that supplies a larger amount of dose at the CAX with respect to the off axis areas. This result is comparable for both 6 and 18 MV but more significantly with 2.5cm Gamma Putty thickness at 18 MV. The majority of dose deposited at the surface

directly under the blocks has been generated by electron contamination. It was also reported that dose from the block tray and air to be the main source of skin dose. This effect was dominant in larger field sizes and high energies. Air between source and skin generates secondary electrons and these electrons absorbed or scattered in air depended on beam divergence and some of them could reach the patient's skin. The impact will become more prevalent as SSD increased and the number of electrons that reach the patient's skin decreased.¹⁴ However, air has more impact than electron contamination.

**Figure 2a:** Gamma Putty Tray factor for different thickness at 18 MV**Figure2b:** Gamma Putty Tray factor for different thickness at 6 MV

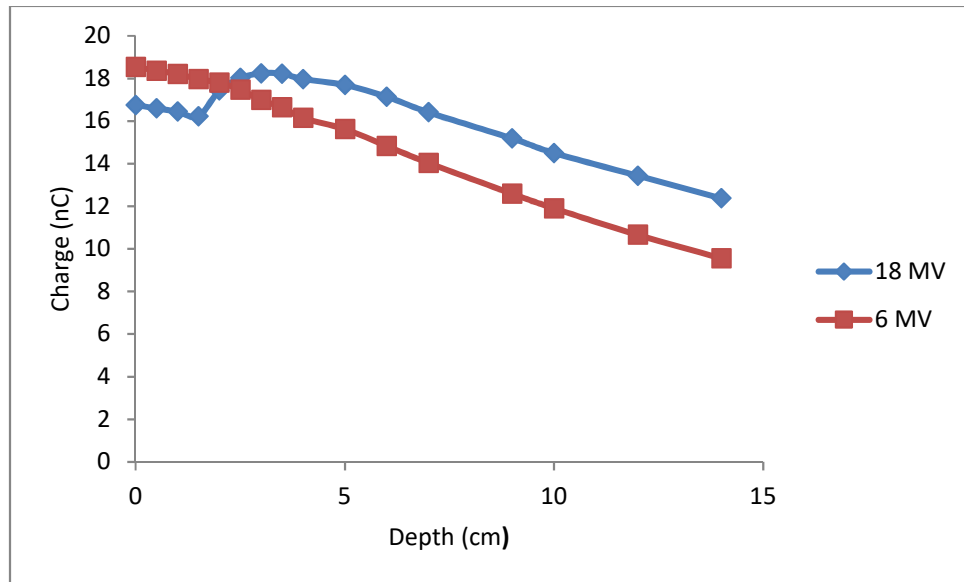


Figure 3a: Ionization depth dose curve without Gamma Putty thickness with 6 and 18 MV photon beam at $10 \times 10 \text{ cm}^2$ field, measured using a Farmer type chamber in solid water phantom.

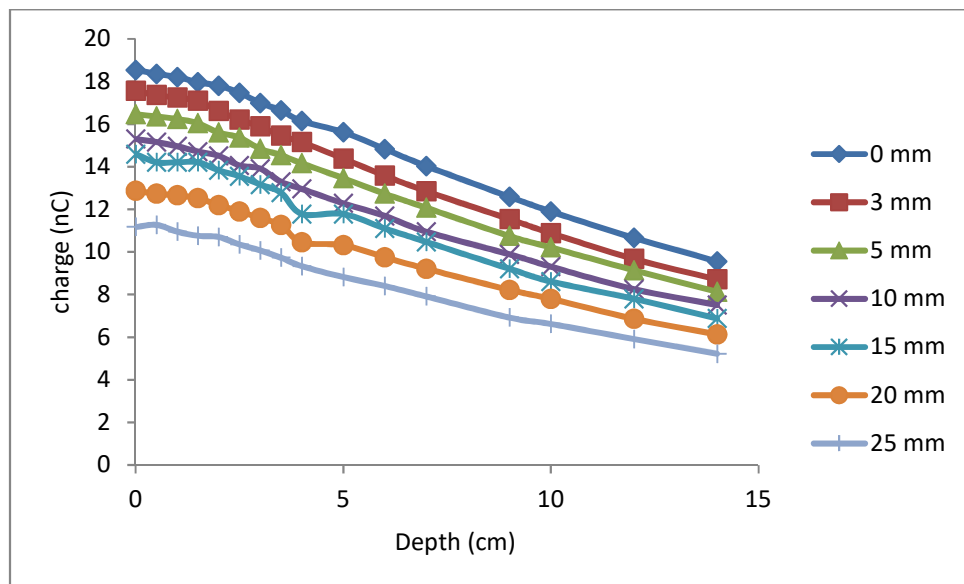


Figure 3b: Ionization depth dose curve for variable Gamma Putty thicknesses block with 6 MV photon beam at $10 \times 10 \text{ cm}^2$ field, measured using a Farmer type chamber in solid water phantom.

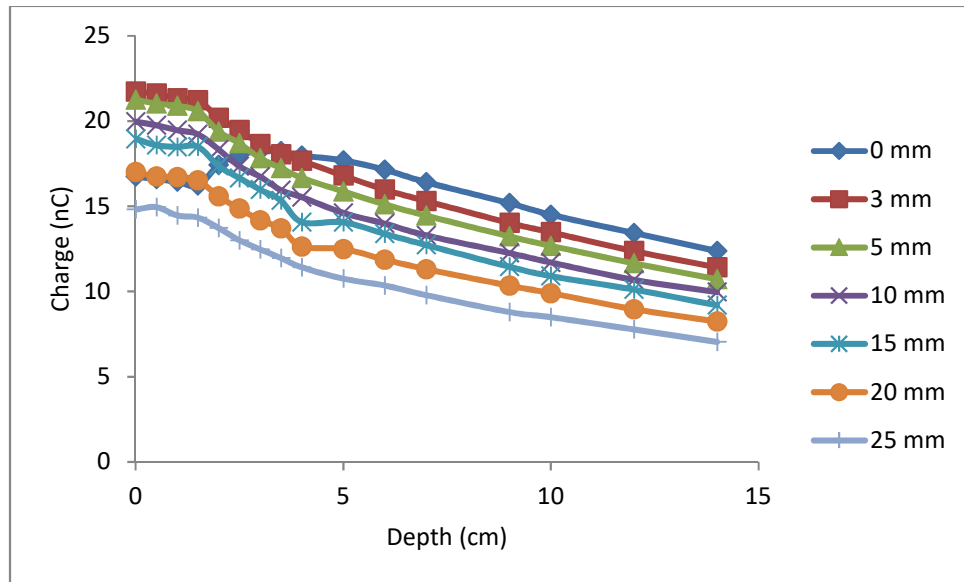


Figure 3c: Ionization depth dose curve for variable Gamma Putty thicknesses block with 18 MV photon beam at 10 × 10 cm² field, measured using a Farmer type chamber in solid water phantom.

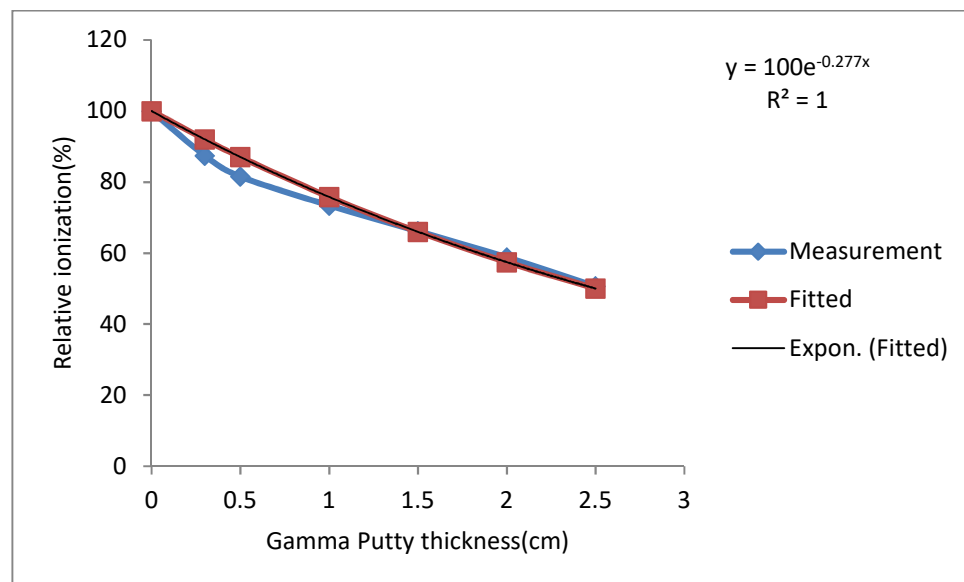


Figure 4a: Attenuation of photon beam intensity with the variation of Gamma Putty block thickness for 6MV

Table 3: Half value and tenth value thickness for Gamma Putty blocks

Field size	Energies			
	6 MV		18 MV	
	HVT (cm)	TVT(cm)	HVT(cm)	TVT(cm)
10X10	2.501	8.312	2.840	9.436
9X9	2.739	9.101	2.899	9.634
8X8	2.484	8.253	2.875	9.554
7x7	2.475	8.223	2.851	9.473
6X6	2.466	8.194	2.840	9.434
5X5	2.466	8.194	2.840	9.434
4X4	2.448	8.136	2.828	9.396
Mean ± std	2.513±0.101	8.350±0.337	2.855±0.024	9.487±0.081
C.V (%)	4.00	4.00	0.80	0.80

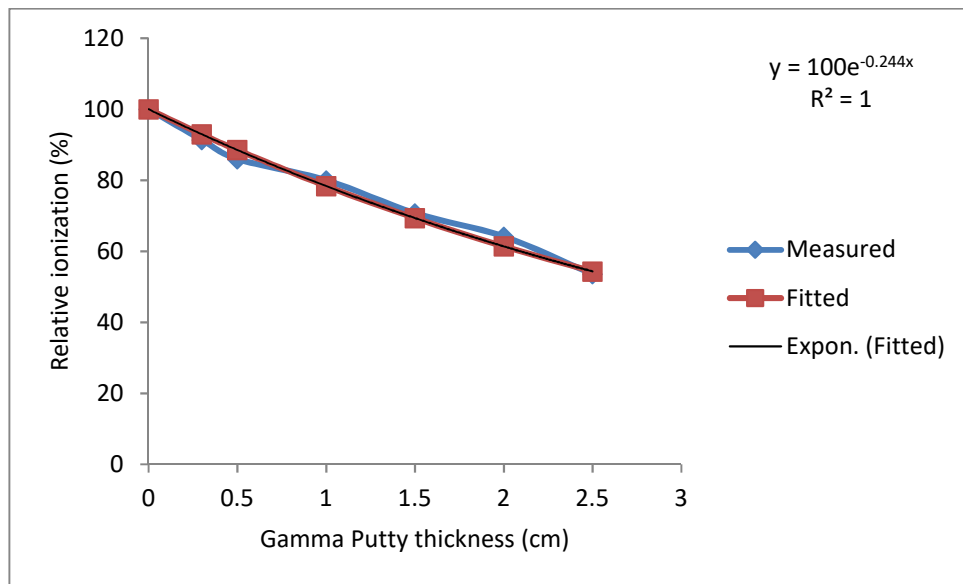


Figure 4b: Attenuation of photon beam intensity with the variation of Gamma Putty block thickness for 18 MV photons.

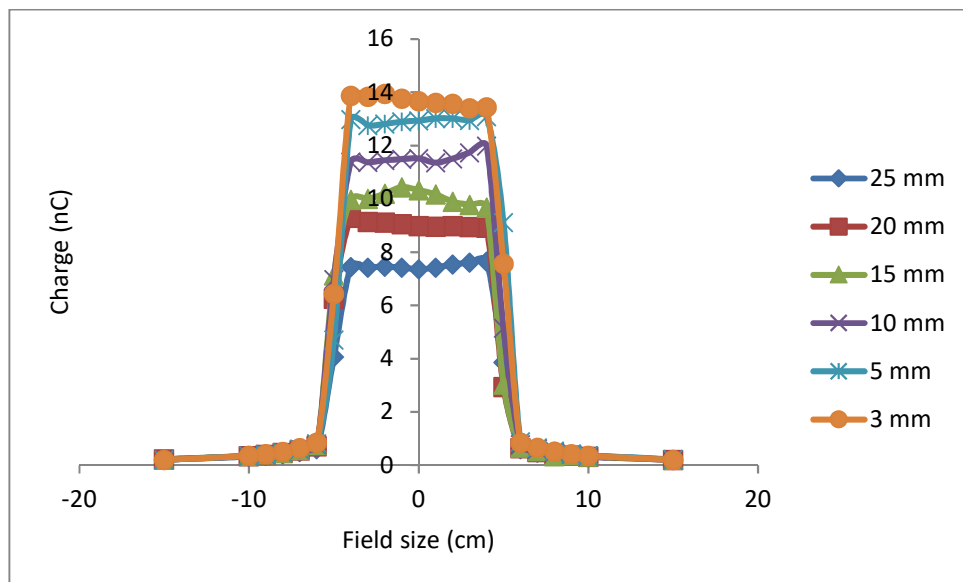


Figure 5a: Off-axis relative dose profile at a depth of 0.5 cm for a 10 x 10 cm² field size at 6 MV and 100 cm SSD

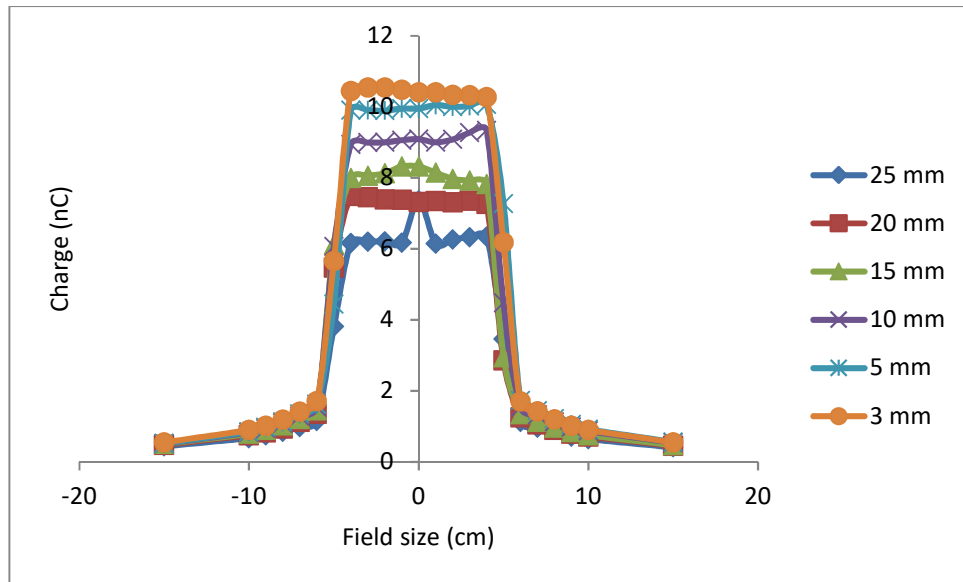


Figure 5b: Off-axis relative dose profile at a depth of 0.5 cm for a 10 x 10 cm² field size at 18 MV and 100 cm SSD

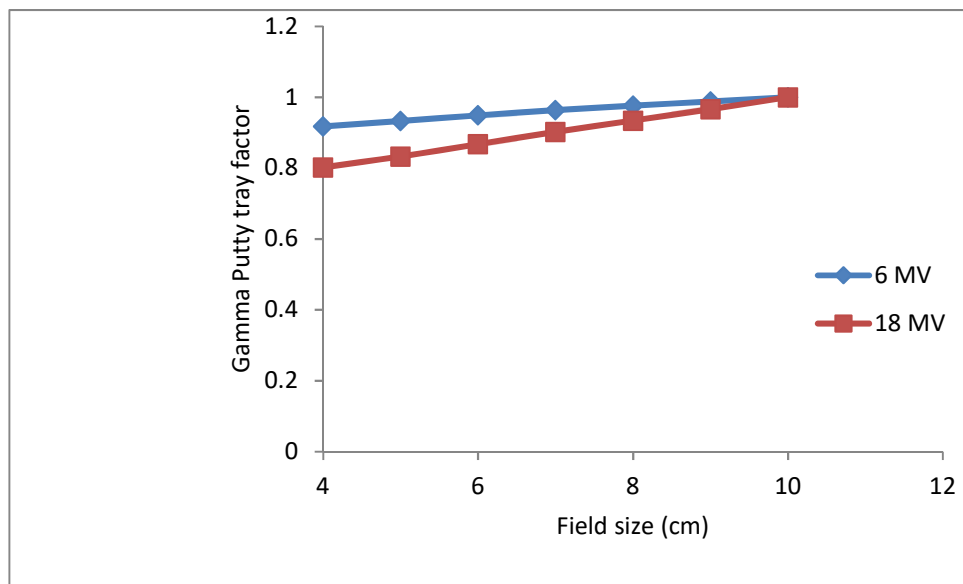


Figure 6a: Surface dose as a GPTF at 0 mm depth for 18 and 6 MV beam. GPTF is shown as a function of the Gamma Putty thickness.

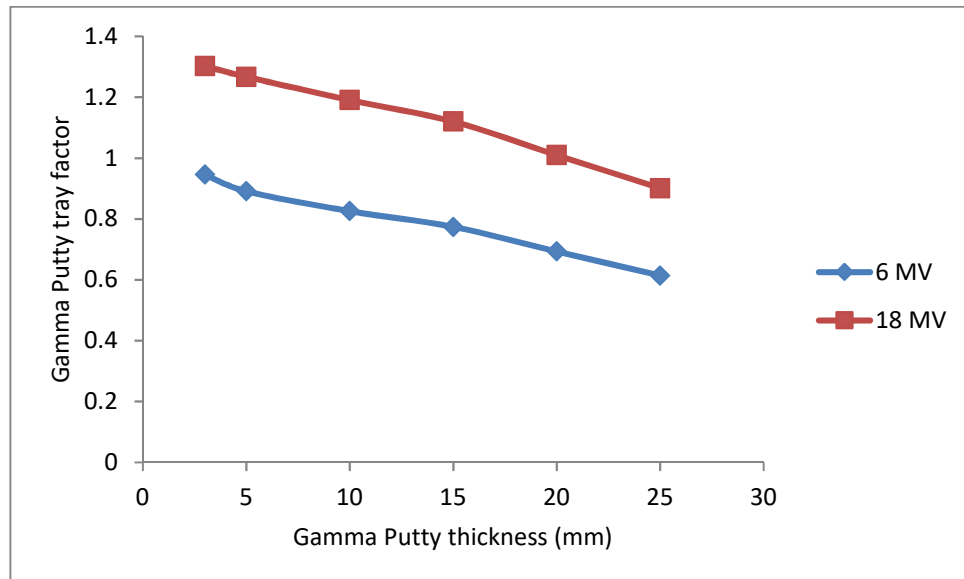


Figure 6b: Surface dose as a GPTF at 5 mm depth for 18 and 6 MV beam. GPTF is shown as a function of the Gamma Putty thickness.

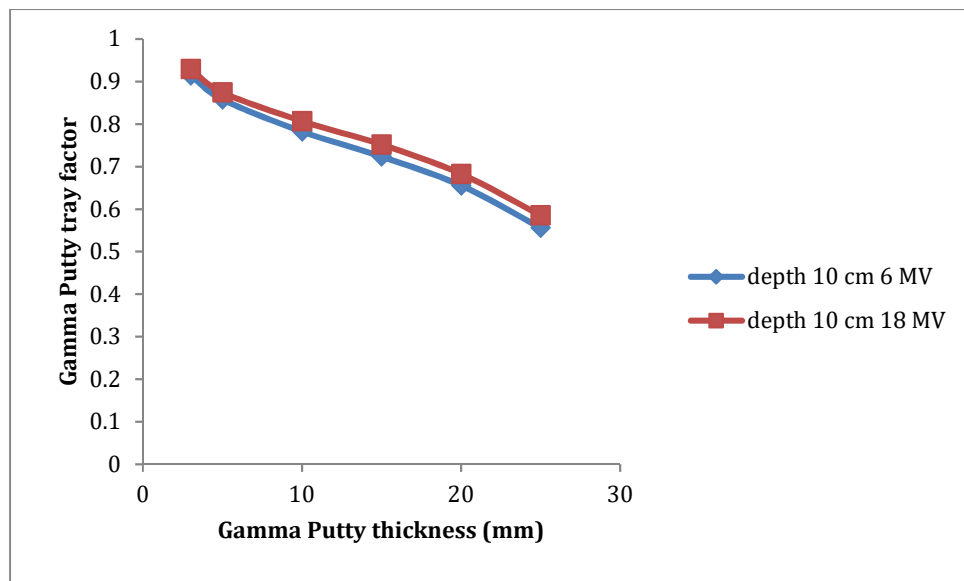


Figure 6c: Surface dose as a GPTF at 10 cm depth for 18 and 6 MV beam. GPTF is shown as a function of the Gamma Putty thickness.

3.4. Surface dose

Surface dose is usually defined as percent depth dose at 0.5 mm depth, with normalization to d_{max} . Similarly to a block tray, Gamma Putty increases skin dose. The effect is stronger with increasing field size and decreasing Gamma Putty thickness. Skin dose values with the Gamma Putty block were higher than those with an open field by comparing GPTF of Figures 6a, b, and c. The effect was dominant in larger field sizes as the Gamma Putty eliminates electrons from upstream and generates new secondary electrons by itself.¹⁵ These results in

higher number of electrons created than eliminated. In addition, secondary electrons initiated at the Gamma Putty can reach the patient, thus increasing the skin dose more significantly. The effect is exacerbated from the upper and lower windows in addition to the impact of SSD, field size, and energy. Figures 6b and c shows the measured surface dose as a function of GPTF taken at 5 mm depth. The surface dose decreases with Gamma Putty thickness due to the beam hardening effect. The reduction is about 6%, 14.5%, 22%, 36.37%, and 54%,

for 6 MV and 2.75 %, 9.36%, 16.2%, 28.95%, and 44.47% for 18 MV for Gamma Putty thicknesses of 0.3, 0.5, 1.0, 1.5, 2.0, and 2.5 cm, respectively. This demonstrates the impact of beam hardening on the surface dose. All these factors enumerated above such as contaminant electrons generated by the collimator, interactions of photons with Gamma Putty, self-absorption of Gamma Putty played a major role in dose summation. However, at 10 cm depth interestingly enough, GPTF does not get closer to unity. Hence, for small field size, photons and electrons are scattered out of the field when they pass through the Gamma Putty. Beyond d_{max} , the factor nearly remains constant.

4. Conclusion

In this report, Gamma Putty shielding effect on the megavoltage photon beam output has been analyzed for F18 and 6 MV. The result showed that several parameters are responsible for fluctuation of dose received by a point in air blocked by a Gamma Putty. They included: field size, thickness of the attenuator, and beam energy. The impact of these parameters is heightened by electrons contamination with increasing field sizes and beam energy. In addition, the measurement showed that GPTF values decreased with increasing field size, depth, and thickness as beam hardening and more scatter for larger field sizes contributed to dose at the given depth. The study revealed that the dose outside the field are governed by the skin collimation stopping the electrons in the incident beam due to the presence of the Gamma Putty shielding and increased lateral scatter of the photon beam as the Gamma Putty thickness is increased. Furthermore, the study suggested that contaminant electrons to be a major factor of dose outside the field at shallow depths. The magnitude and extent increased with beam energy, even more in the presence of beam modifiers. In general, the primary dose rate at shallow depths in the phantom may actually increase at distances away from the CAX due to flattening filter effects on the radiation beam.^{16,17}

Regarding the results, the percent ionization depth dose was measured in solid water with broad beam geometry. Solid Water is convenient as it eliminates transport, rigorous set-up, and water filling tanks. However, the uncertainties budget for the measurement include difference of stopping power of solid water that amount to 4% less than that of water between 10 keV and 50 MeV,¹⁸ temperature differential between treatment rooms and solid water, and several correction factors derived from temperature and pressure, ion chamber, electrometer, and absolute calibration. In addition, systematic error from set-up including tight fit for ion chamber, thermal equilibrium with the temperature in the cavity, and acrylic holder may play a major role in the data collected. Finally, the need to maintain a consistency with regard to compressibility and pressure

in the confection of the Gamma Putty samples need to be explored.

Conflict of Interest

The authors declare that they have no conflicts of interest. The authors alone are responsible for the content and writing of the paper.

References

1. Matsumoto Y, Umezu Y, Fujibuchi T, *et al.* Verification of the protective effect of a testicular shield in postoperative radiotherapy for seminoma. *Nihon Hoshasen Gijutsu Gakkai Zasshi*. 2014;70(9):883-7.
2. Craciunescu OI, Steffey BA, Kelsey CR, *et al.* Renal shielding and dosimetry for patients with severe systemic sclerosis receiving immunoablation with total body irradiation in the scleroderma: cyclophosphamide or transplantation trial. *Int J Radiat Oncol* 2011;79(4):1248-55.
3. Purdy JA, Stiteler RD, Glasgow GP, *et al.* Gonadal shield Radiology. 1975;117-226.
4. Sohn JW, Macklis R, Suh JH, *et al.* A mobile shield to reduce scatter radiation to the contralateral breast during radiotherapy for breast cancer: preclinical results. *Int J Radiat Oncol Biol Phys*. 1999;43(5):1037-41.
5. Toljanic JA, Saunders VW Jr. Radiation therapy and management of the irradiated patient. *J Prosthet Dent*. 1984;52:852-8.
6. Mantri SS, Bhasin AS, Shankaran G, *et al.* Scope of prosthodontic services for patients with head and neck cancer. *Indian J Cancer*. 2012;49:39-45.
7. Prabhakar R, Haresh KP, Sridhar PS, *et al.* Execution of mantle field with multileaf collimator: a simple approach. *J Cancer Res Ther*. 2008;4(1):18-20.
8. Shiu AS, Tung SS, Gastorf RJ, *et al.* Dosimetric evaluation of lead and tungsten eye shields in electron beam treatment. *Int J Radiat Oncol Biol Phys*. 1996;35:599-604.
9. Rustgi SN. Dose distribution under external eye shields for high energy electrons. *Int J Radiat Oncol Biol Phys*. 1986;12:141-4.
10. Weaver RDS, Gerbi BJ, Dusenbery KE. Evaluation of eye shields made of tungsten and aluminum in high-energy electron beams. *Int J Radiat Oncol Biol Phys*. 1998;41:233-7.
11. Xu T, Shikhaliyev PM, Al-Ghazi M, *et al.* Reshapable physical modulator for intensity modulated radiation therapy. *Med Phys*. 2002;29:2222-9.
12. Jiang SB, Ayyangar KM. On compensator design for photon beam intensity-modulated conformal therapy. *Med Phys*. 1998;25:668-75.

13. Du Plessis FCP, Willemse CA. Monte Carlo calculation of effective attenuation coefficient for various compensator materials. *Med Phys.* 2003;30:2537-43.
14. Khan FM. The physics of radiation therapy, Williams and Wilkins, Baltimore. 1994:323-32.
15. Kim S, Liu CR, Zhu TC, *et al.* Photon beam skin dose analyses for different clinical setups. *Med Phys.* 1998;25: 860-6.
16. Thomas SJ, Thomas RL. A beam generation algorithm for linear accelerators with independent collimators. *Phys Med Biol.* 1990;35(3):8.
17. Kwa W, Kornelsen RO, Harrison RW, *et al.* Dosimetry for asymmetric x-ray fields. *Med Phys.* 1994; 21(10):1599-604.
18. Ramaseshan R, Kohli K, Cao F, *et al.* Dosimetric evaluation of Plastic Water Diagnostic-Therapy. *J Appl Clin Med Phys.* 2008;9(2):2761.